Investigations of the Mechanisms that Govern Carbon Dioxide Sequestration via Aqueous Olivine Mineral Carbonation

CONFERENCE PAPER *in* FUEL AND ENERGY ABSTRACTS · JANUARY 2003

CITATIONS
3

READS
7

6 AUTHORS, INCLUDING:

Hamdallah Bearat
An-Najah National University
44 PUBLICATIONS **580** CITATIONS
SEE PROFILE

Ray W. Carpenter
Arizona State University
158 PUBLICATIONS **1,617** CITATIONS
SEE PROFILE

Investigations of the Mechanisms that Govern Carbon Dioxide Sequestration via Aqueous Olivine Mineral Carbonation

Hamdallah Béarat,[#] Michael J. McKelvy,*[#] Andrew V.G. Chizmeshya,* Ryan Nunez, [#] and R.W. Carpenter*[#]

**Center for Solid State Science and [#]Science and Engineering of Materials Graduate Program*
Arizona State University, Tempe, Arizona 85287 USA

ABSTRACT

Coal, in particular, and fossil fuels, in general, are well positioned to supply the world's energy needs for centuries to come *if* the environmental challenges associated with anthropogenic carbon dioxide emissions can be overcome. Carbon dioxide sequestration is being actively pursued as an option to reduce CO_2 emissions, while still enjoying the advantages of low-cost fossil fuel energy. Mineral carbonation is an intriguing CO_2 sequestration candidate technology, which provides environmentally benign and geologically stable CO_2 disposal in the form of mineral carbonates. Importantly, such disposal bypasses many long-term storage problems by (i) providing permanent containment, (ii) avoiding adverse environmental consequences, and (iii) essentially eliminating the need for continuous site monitoring. The primary challenge for viable sequestration process development is reducing process cost. Enhancing carbonation rates is crucial to reducing cost. This is the primary focus of the CO_2 Mineral Sequestration Working Group managed by Fossil Energy at DOE.

Carbonation of the widely occurring mineral olivine (e.g., forsterite, Mg_2SiO_4) is a leading process candidate, which converts CO_2 into the environmentally benign mineral magnesite ($MgCO_3$). As olivine carbonation is exothermic, it offers intriguing low-cost potential. Recent studies at the Albany Research Center have found aqueous-solution carbonation is particularly promising. Cost-effectively enhancing carbonation reactivity is central to reducing process cost. Many of the mechanisms that impact reactivity occur at the solid/solution interface. Understanding these mechanisms is central to the engineering of processes to enhance carbonation reactivity and lower cost. Herein, we describe our investigations of mineral carbonation reaction mechanisms for a model phase-pure olivine. Aqueous-solution olivine carbonation was discovered to be a complex process associated with passivating silica layer formation and cracking, silica surface migration, olivine etch pit formation, transfer of the Mg and Fe in the olivine into the product carbonate, and the nucleation and growth of magnesite crystals on/in the silica/olivine reaction matrix. These phenomena occur in concert with the large solid volume changes that accompany the carbonation process, which can substantially impact carbonation reactivity.

INTRODUCTION

Worldwide energy consumption is increasing exponentially, driven by the rising global standard of living.[1,2] As developing countries strive to attain the quality of life enjoyed by developed countries, the already increasing demand for low-cost energy is likely to accelerate even further. Although the global energy infrastructure enjoys a diverse portfolio of technologies, fossil fuels currently supply 85% of world energy needs. Coal feeds a large fraction of this demand, due its wide availability, high energy density and low cost. Known coal reserves alone are sufficient to

satisfy global energy demands for centuries to come, if the environmental concerns associated with anthropogenic CO_2 emissions can be overcome.[1-5] These concerns can have a major impact on the balance of technologies used for future energy generation, as fossil-fuel combustion is the major anthropogenic source of CO_2 emissions. The concerns are particularly important to the coal industry, as coal emits particularly high levels of CO_2 during energy generation.[1,2,6]

Two alternatives for mitigating anthropogenic CO_2 emissions are available: (i) alternative energy sources can provide CO_2-free energy or (ii) fossil-fuel energy generation can be coupled with CO_2 sequestration.[6] As the world's energy infrastructure is heavily dependent on fossil-fuel energy, alternative energy technologies are unlikely to satisfy global energy demands in the foreseeable future.[1,2] CO_2 sequestration provides an important alternative.[1,2,6] Several candidate technologies are being explored, including useful materials conversion using CO_2 and terrestrial, geological, and ocean sequestration. Successful technologies need to (i) be environmentally benign, (ii) provide a permanent solution, and (iii) be economically viable.

Unlike other candidate technologies, which propose long-term storage (e.g., ocean and geological sequestration), CO_2 mineral sequestration provides permanent CO_2 disposal by forming geologically stable mineral carbonates.[2,7,8] The materials formed already exist in vast quantities in nature, in locations such as Grand Canyon Park, Arizona, underscoring the potential for environmentally benign sequestration.[8] As mineral carbonation has the inherent potential to be permanent and environmentally benign, the remaining goal is economically viable process development. Process costs can be considered in two categories: (i) the initial cost of capture and sequestration and (ii) the ongoing costs associated with guaranteeing long-term storage. Mineral carbonation offers substantial advantages that minimize the latter costs. As the carbonates that form (e.g., $MgCO_3$ and $CaCO_3$) are both thermodynamically and geologically stable, they essentially offer permanent CO_2 disposal, which provides substantial ongoing cost advantages. In particular, mineral carbonation avoids or greatly reduces the ongoing costs associated with long-term storage, including the costs associated with (i) continuous site monitoring, (ii) liability issues (e.g., litigation and insurance costs associated with sudden CO_2 release), and (iii) sequestering higher levels of CO_2 to offset any leakage from long-term storage. Consequently, the primary research focus is on evaluating the potential to lower the cost of the mineral carbonation process. This is the goal of the CO_2 Mineral Sequestration Working Group managed by DOE/Fossil Energy, which includes members from the Albany Research Center (ARC), Los Alamos National Laboratory, the National Energy Technology Laboratory, Science Applications International Corp., and our research group at Arizona State University (ASU).

Mineral carbonation of Mg-rich olivine minerals (e.g., forsterite, Mg_2SiO_4) is a leading CO_2 sequestration process candidate.[9,10] These minerals are widely available in readily mineable deposits worldwide, providing the capacity to sequester at least a substantial fraction of the CO_2 that can be generated from global coal reserves.[8] Their low-cost, combined with the exothermic nature of the carbonation process (reaction 1),[8] provide exciting potential for economically

$$(1) \qquad \tfrac{1}{2}Mg_2SiO_4 + CO_2 \rightarrow MgCO_3 + \tfrac{1}{2}SiO_2 + 88\ kJ/mol$$

viable process development. Recent ARC studies[9,10] indicate aqueous solution carbonation is particularly promising. Key to lowering process cost is increasing the carbonation reaction rate

and enhancing its degree of completion. These have been found to vary substantially depending on the olivine feedstock, how it is pretreated, and the reaction conditions used. The available studies for this complex process show it to be promising, but far from optimized.[9,10] Enhancing the reaction rate and degree of completion (i.e., carbonation reactivity) are essential to minimizing process cost. Herein, we describe our initial investigations into the reaction mechanisms that govern the olivine mineral carbonation process. The goal is to develop the necessary scientific understanding to facilitate the engineering of new materials and processes that can enhance carbonation reactivity and lower process cost.

EXPERIMENTAL

Feedstock Characterization: A variety of olivine, $(Mg_xFe_{1-x})_2SiO_4$, materials from different sources were structurally and compositionally characterized (e.g., via X-ray powder diffraction, field-emission scanning electron and optical microscopy, and electron microprobe and particle induced X-ray emission elemental analysis) to identify model materials with high phase and compositional purity. Two olivine materials, which primarily differ in their iron content, from San Carlos, Arizona, were selected as the model materials for investigation. One is light green (LG), while the other is gray green (GG). Their elemental compositions were determined to be LG: $(Mg_{0.92}Fe_{0.08})_2SiO_4$ and GG: $(Mg_{0.83}Fe_{0.17})_2SiO_4$ by electron microprobe and particle induced X-ray emission analysis. Energy dispersive X-ray spectroscopy (EDS) was coupled with field-emission scanning electron microscopy to probe the olivine compositions at the microscale, as shown for the LG olivine in Figure 1. X-ray powder diffraction (XPD) was used to structurally characterize the starting materials. Both materials are phase pure, as seen in Figure 2. The lattice constants are in good agreement with those observed for olivine LG (a = 4.763 Å, b = 10.223 Å, c = 5.993 Å) and GG (a = 4.766 Å, b = 10.243 Å, c = 5.999 Å).[11,12] Each of the trace impurities observed for both materials were well below 1%, with Ca being the principle trace impurity. Single crystals, single crystal fragments, and, occasionally, polycrystalline materials were investigated. Studies to date have principally focused on the LG olivine, which is similar in composition to the Twin Sisters olivine being investigated at the ARC.[9,10] The GG (17% Fe) olivine is currently being investigated to explore the effects of Fe substitution.

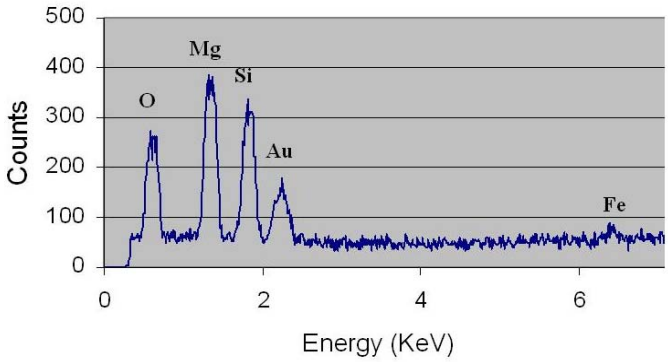

Figure 1. Typical energy dispersive X-ray spectrum for the LG olivine feedstock showing the low-level of Fe present. The gold peak results from gold coating the sample to minimize charging in the FESEM.

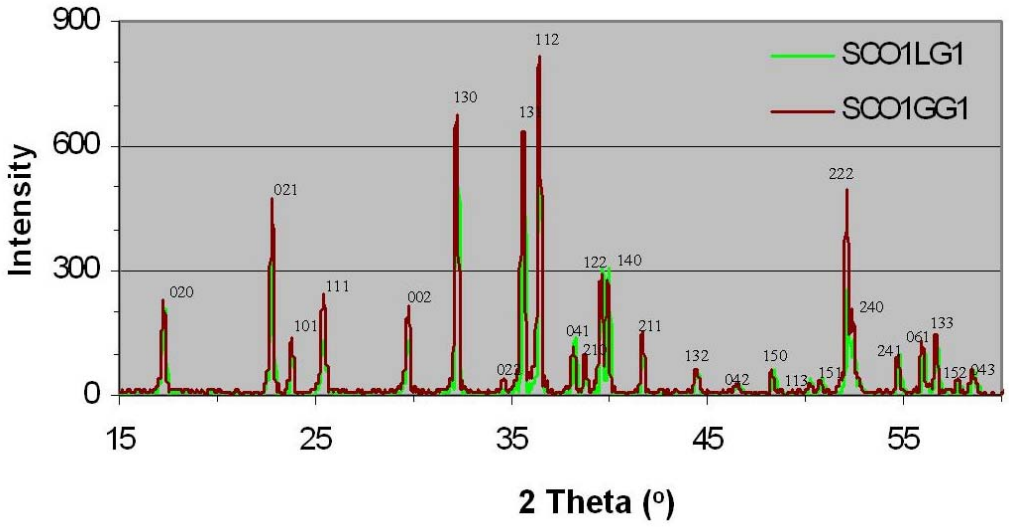

Figure 2. X-ray powder diffraction patterns for the model olivine feedstock materials. Both materials are from San Carlos, Arizona. The green pattern corresponds to the LG olivine (SCO1LG1) and the red-brown pattern to the GG olivine (SCO1GG1). The reflections are indexed as shown. Note the slight shift of gray green reflections to lower angles, consistent with the slight increase in cell parameters expected for higher Fe concentrations in olivine.

The reaction conditions employed are the same as those used in the ARC process, as summarized below for forsterite, to facilitate direct integration of the mechanistic studies herein with the process development research being carried out at the ARC.[10] The reactions were carried out

$$Mg_2SiO_4 + 2CO_2 \xrightarrow[0.64\ M\ NaHCO_3,\ 1M\ NaCl]{\sim 185\ ^oC,\ \sim 150\ atm\ CO_2} 2MgCO_3 + SiO_2$$

for a variety of particle sizes and reaction times to probe the intermediate reaction materials that form. Aggressive stirring was generally employed (1,000 to 2,000 rpm) to further replicate the actual ARC process. The carbonation feedstock typically contained equal amounts by weight of largely single crystal LG olivine fragments in the size ranges -37μ and 37 to 200 μ. Larger single crystal fragments were occasionally reacted to investigate the intermediate materials that form over larger regions. Select samples for cross-section transmission electron microscopy analysis of the surface reaction interface region were subjected to carbonation reaction conditions identical to those above, but without stirring. These runs were employed to better preserve the reaction interface region by avoiding any mechanical surface abrasion that may occur during stirring. The mineral carbonation system employed is an Autoclave Engineers EZE-Seal Hastelloy C-276 reaction system. The system employs essentially the same design as the reactor being used at the Albany Research Center. The principle difference is the reaction volume. The ASU system incorporates a substantially smaller volume (100ml vs. 2 liters at the ARC), to better accommodate the smaller sample sizes used herein. Comparative carbonation runs in both systems using the same Twin Sisters olivine feedstock[13] gives essentially the same extent of carbonation (36 ± 3%), which (i) indicates similar reaction conditions are present in both systems using the standard conditions above and (ii) allows direct comparison of the present mechanistic studies with current process development investigations at the ARC.

The partially carbonated reaction products were analyzed structurally, morphologically and analytically to probe the mechanisms that govern the mineral carbonation reaction process. X-ray powder diffraction patterns were obtained for the carbonation products using a Rigaku D/MAX-IIB X-ray diffractometer with Cu$K\alpha$ radiation. Scans were taken over different 2θ ranges between 10º to 70º, with steps of 0.01º/s. Partially carbonated reaction products were imaged using a Hitachi 4700 field-emission scanning electron microscope (FESEM). Elemental analysis of individual reaction product particles was accomplished via energy dispersive X-ray spectroscopy (EDS) using a EDAX Phoenix system coupled with the Hitachi 4700. Cross-sectioned samples of the reaction interface were imaged by transmission electron microscopy, using a FEI CM200-FEG. The extent of carbonation and nature of the silica-rich by-product (e.g., is the silica formed primarily SiO_2 or is it partially hydroxylated) that forms during carbonation were assessed using a Perkin Elmer Series II CHNS Analyzer. Comparative standards gave total carbon and hydrogen accuracies of ± 0.3 wt%.

EXPANSION AND CONTRACTION OF THE REACTION MATRIX DURING OLIVINE MINERAL CARBONATION

Olivine, $(Mg_xFe_{1-x})_2SiO_4$, forms a solid solution series between its end members forsterite (Mg_2SiO_4) and fayalite (Fe_2SiO_4), with naturally occurring olivine being generally richer in magnesium.[14] It adopts the orthorhombic structure shown in Figure 3. The cell parameters observed generally increase with increasing Fe substitution in the solution series, exhibiting Vegard-like behavior between the forsterite and fayalite end members (e.g., Mg_2SiO_4: a = 4.76Å, b = 10.20 Å, and c = 5.98 Å; Fe_2SiO_4: a = 4.82 Å, b = 10.48 Å, c = 6.11 Å).[14]

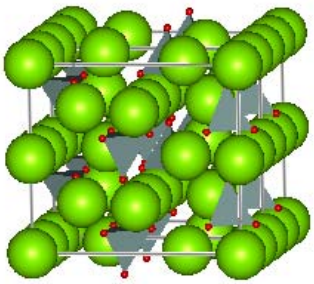

Figure 3. The orthorhombic structure of olivine. The Mg/Fe positions are shown as green spheres. The silica tetrahedra are represented by the gray tetrahedra with the small red spheres representing the oxygen atom positions.

Volume change is likely a key parameter associated with the olivine mineral carbonation process. For example, magnesite formation from forsterite [reaction (1)] is associated with a 30% volume increase (comparing the volume of the $2MgCO_3$ formed per Mg_2SiO_4). On the other hand, the silica produced during carbonation is expected to exhibit a substantial volume decrease of ~38% (estimated using the density of vitreous silica) compared with Mg_2SiO_4. As Fe is substituted for Mg in olivine, little change is expected in the relative molar volumes of the associated olivine, carbonate and silica, as the product volume of $FeCO_3$ (siderite) is expected to be 30% greater than that of Fe_2SiO_4 (fayalite), while the product volume of silica is estimated to

be ~ 42% less than that for fayalite.[15] This suggests that the olivine reaction matrix may undergo substantial expansive and compressive stress during the formation of the carbonate and silica, respectively. Such forces appear to play an important role during mineral carbonation, as discussed below.

RESULTS AND DISCUSSION

XPD indicates the only crystalline product that forms during olivine mineral carbonation is magnesite, as shown in Figure 4. This suggests any silica-containing reaction products are poorly ordered (essentially amorphous) in character. The cell parameters observed for magnesite are slightly greater than those observed for pure $MgCO_3$, suggesting that the product magnesite contains some (~10%) Fe substitution for Mg based on Vegard's Law.[16] The following paper presents a first principles computational modeling study of the thermodynamics and structural behavior of the product carbonate as a function of the extent of Fe/Mg substitution, which facilitates direct comparison of the Fe content of the product carbonate with its cell parameters.[17]

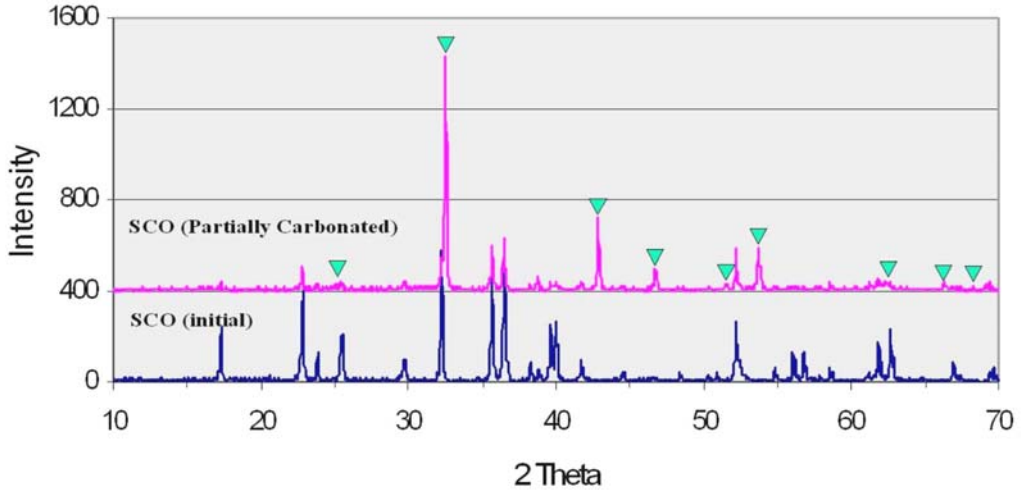

Figure 4. X-ray powder diffraction analysis showing the only crystalline product formed during mineral carbonation is magnesite. A slight increase in the cell parameters above those typically observed for magnesite is generally observed, suggesting at least some Fe is transferred from the olivine feedstock into the product magnesite during carbonation. The major product magnesite peaks are identified by the green triangles.

Figure 5 shows a FESEM image and EDS analysis of typical product materials that form during mineral carbonation. The products generally consist of crystals intergrown with an irregularly shaped product matrix. Energy dispersive X-ray spectroscopy (EDS) for Mg, Si, and O (up to 5 keV) shows the crystals exhibit the strong Mg and O signals expected for magnesite, while the irregularly shaped matrix exhibits the strong Si and O signals expected for silica, consistent with reaction (1). Higher energy EDS analysis confirmed that Fe is carried into the magnesite during carbonation, as suggested by XPD above, leaving the product silica essentially Fe free (see below). C and H elemental analysis of the reaction products shows the extent of carbonation is 49%, and at least the majority of the product formed is H free (within experimental error ± 0.3 wt.%). Together with the lack of observation of any crystalline product material other than magnesite by XPD, this indicates the majority of the silica formed is amorphous SiO_2.

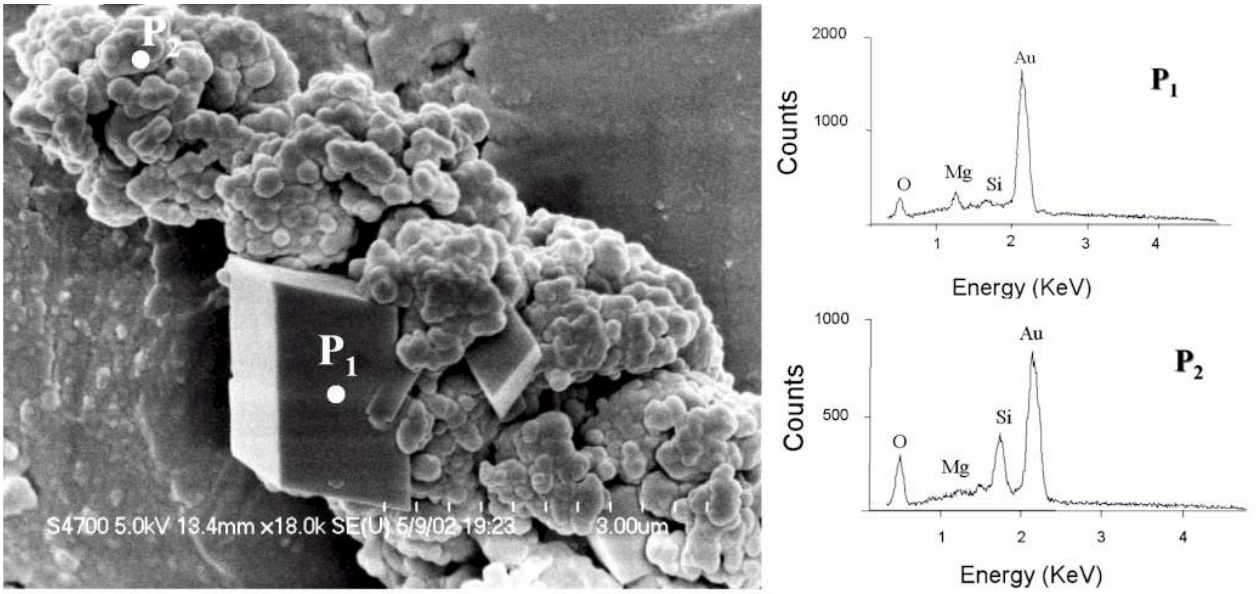

Figure 5. FESEM image and energy dispersive X-ray spectra (EDS) of the olivine carbonation reaction products. A strong Mg and O signal is associated with the product crystals (P_1), whereas a strong Si and O signal is associated with the irregular habited product material (P_2). Note: due to the small size of the particles observed, there is a slight overlap of the EDS scattering volume between the irregularly shaped and crystalline particles. The gold peak is associated with gold coating of the sample to minimize charging.

Figure 6 shows a representative example of the intergrowth of olivine, silica and magnesite found in the mineral carbonation reaction products for a reaction that exhibited a 50% extent of carbonation. The appearance of abrasive wear on the outside corners of the magnesite crystals on the surface of the reaction matrix is of particular interest, as it indicates the olivine/silica/magnesite intergrowth observed is representative of a material that forms during mineral carbonation. This follows from the high stirring speed used during mineral carbonation,

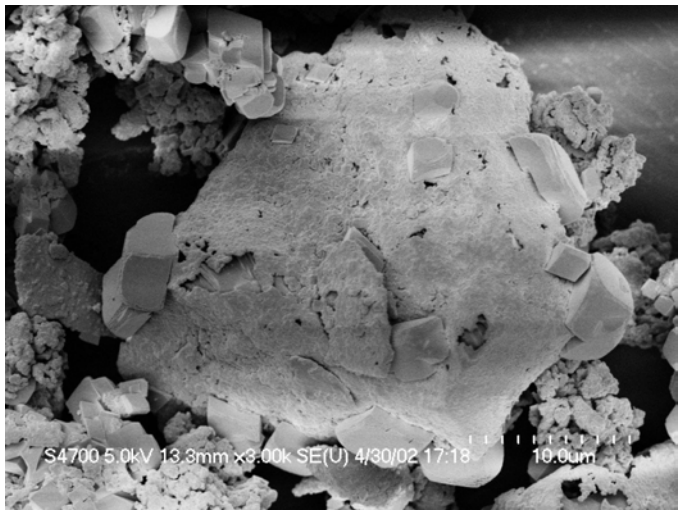

Figure 6. FESEM image of the frequently observed intergrowth between olivine, amorphous silica and the magnesite crystal reaction products. Note the selective appearance of abrasive wear on the outside corners of the magnesite crystals that have grown on the surface of the olivine/silica/magnesite reaction matrix.

which facilitates abrasive collisions, resulting in the preferential wearing of the outside corners of the magnesite crystals that have grown on the surface of the olivine/silica reaction matrix. Such preferential wear would not be present if the intergrowths formed as aggregates of independent particles that settled out upon reaction completion. The intergrowth of the magnesite crystals with the olivine/silica reaction matrix shown in Figure 7 suggests that magnesite can grow into, as well as away from, the olivine/silica reaction matrix surface.

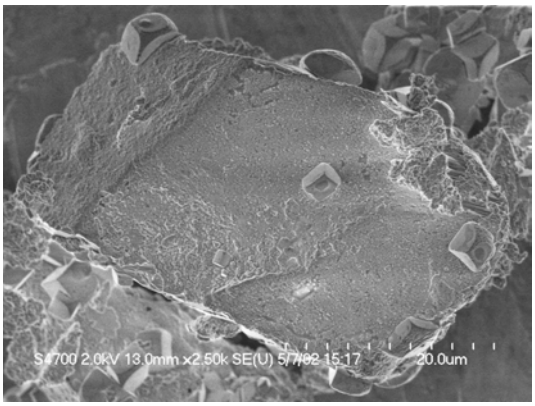

Figure 7. A FESEM image showing the intergrowth of magnesite crystals with the olivine/silica mineral carbonation reaction matrix. Note, in particular, the magnesite crystal in the upper left, which is clearly rooted in the olivine rich region of the reaction matrix, suggesting it was growing into, as well as away from, the olivine/silica reaction matrix surface during mineral carbonation.

Figure 8 shows the passivating silica layers that can form on the olivine reaction surface early in the carbonation process. These samples were prepared to retain intact the surface reaction layers that form during mineral carbonation by eliminating the stirring component of the mineral carbonation process, which induces abrasive wear, as seen in Figures 6 and 7. Although the passivating surface layers can be very effective locally at reaction passivation (Figure 8b), the volume contraction associated with silica formation can disrupt/crack the silica layer surface (Figure 8a) facilitating carbonation deeper into the olivine/silica reaction matrix. Such silica layer cracking is key for enhancing olivine carbonation reactivity as the passivating layer regions between the cracks (Figure 8b) can be very long lived.

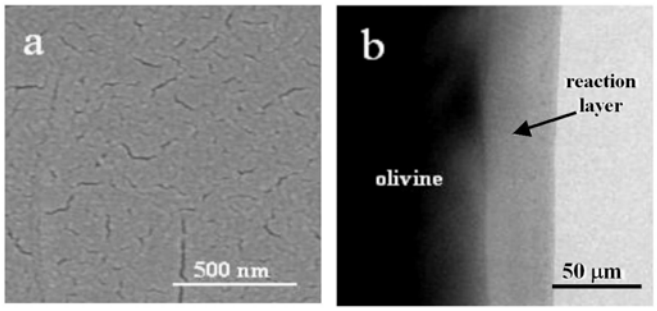

Figure 8. a) FESEM image of passivating silica layer formation on an olivine single crystal surface that formed during unstirred carbonation. The irregular surface can be associated with the shrinking and cracking of the surface silica layer as it forms on the host olivine. b) a cross-section HRTEM image of the same silica reaction layer between the cracks. These layers are slow growing and can effectively passivate the carbonation process locally.

Figure 9 shows the typical inward progression of the carbonation reaction from the olivine surface for the stirred mineral carbonation process. The outer reaction layer structurally disrupts the reaction interface layer *prior to* reaction penetration, which may be related to the volume expansion of the product carbonate compared to the host olivine. This observation underscores the key role structural disruption can play in enhancing carbonation reactivity, especially given how effective silica layer formation can be at local reaction passivation. The intergrowth of silica and magnesite can be clearly seen in the reaction layer via the Si and Mg EDS maps. The Mg and Fe maps demonstrate a strong correlation between Mg and Fe both in the olivine feedstock and product magnesite in the reaction layer, confirming the Fe in the olivine feedstock is carried into the product carbonate during carbonation. By comparison, the silica–rich regions are largely Fe free.

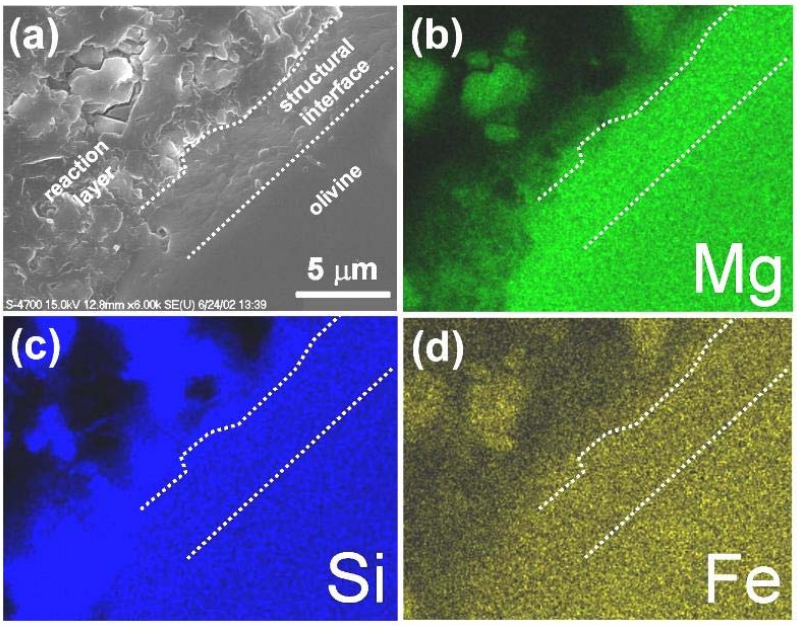

Figure 9. a) FESEM secondary electron image of a cross-section of a partially carbonated olivine single crystal showing the structural disruption that accompanies the mineral carbonation process as the reaction front penetrates to the crystal interior. The crystal surface is in the upper left corner. b-d) Mg, Si, and Fe EDS maps of the reaction interface cross section.

Figure 10 shows another view of the often-observed intergrowth of magnesite crystals with silica for more mature reaction products. In addition to the above observations, etch pits were occasionally observed on olivine surfaces, indicating crystal defects can facilitate olivine dissolution. Figure 11 shows an example of etch pit formation, which can be associated with such defects (e.g., screw dislocations or impurities in the host olivine crystal). The associated silica formation provides further evidence of silica migration. As no carbonate crystals are observed nearby and the volume of silica in the etch pit is relatively small, it appears Mg and Si dissolution is enhanced at such defect sites. The silica that forms along the internal surface of the etch pits may be associated with a local surface dissolution/precipitation/migration process. Such a process can also explain the apparent surface migration of silica observed for other reaction products.

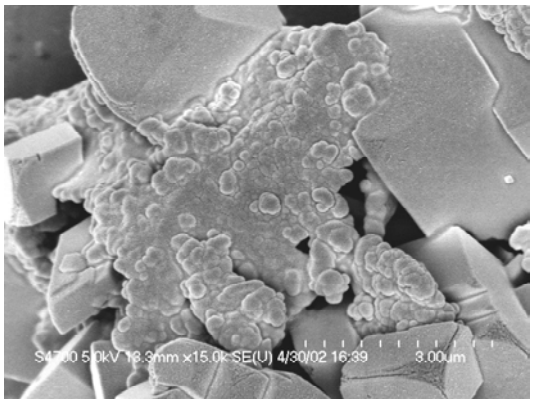

Figure 10. A FESEM secondary electron image of the intergrowth of magnesite crystals and silica for more mature reaction products. Note only the outer edges of the magnesite crystals are abraded, confirming that the reaction matrix formed during *in situ* carbonation and not as the result of particle settling after reaction completion.

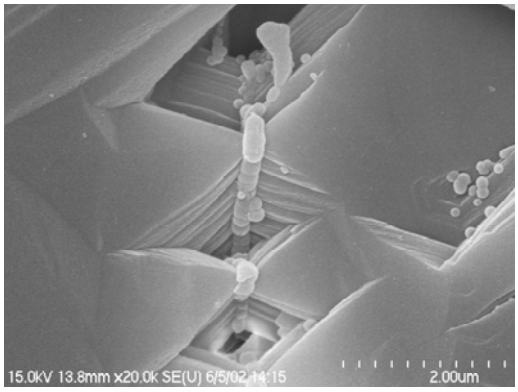

Figure 11. A FESEM secondary electron image of a single crystal olivine surface early in the carbonation process. Note the relatively deep etch pits in the crystal surface, which are related to the observed silica formation (the irregular particles/particle chains within and near the etch pits). The silica that is associated with the pit edges and interior suggests that while magnesium is being lost to solution, some of the silica formed locally migrates along the exposed olivine surfaces.

The relative effectiveness of passivating layer formation is central to olivine mineral carbonation reactivity. To probe the effect of abrasion, e.g., due to particle-particle collisions that may effectively erode away passivating layers as they form, we investigated the extent of carbonation as a function of the % solids used during stirred (1,500 rpm) mineral carbonation. Figure 12 shows the extent of carbonation observed from less than 1% to nearly 20% solids by weight in these initial studies. The maximum extent of carbonation was found to be near 15% solids and drop off substantially for both decreasing and increasing solid levels. The reduction in carbonation observed below 15% solids may be associated with the decrease in particle-particle abrasion effects anticipated for lower particle concentrations. That substantial abrasive wear is present at 15% solids follows from the worn edges observed for the product magnesite crystals (Figures 6 and 7). Future investigations are planned to probe the degree of surface abrasion as a function of decreasing particle concentrations to better understand the impact of abrasion on carbonation reactivity.

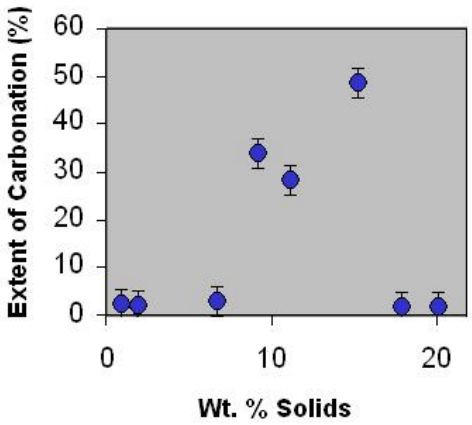

Figure 12. A plot of the extent of carbonation observed as a function of weight % solids during olivine mineral carbonation at 1,500 rpm (180 ^{o}C; 2,200 psi CO_2; 1hr). The error bars show the error associated with the product carbonate analysis.

The origin for the abrupt drop in extent of carbonation for solids levels above 15% might be related to particle agglomeration at higher particle concentrations, as the particle surfaces internal to agglomerates would be shielded from abrasion. Investigations are planned (i) to determine if agglomeration does indeed occur under these conditions and (ii) to confirm that the reaction system still provides full solid/fluid dispersion at these high % solid levels.

CONCLUSIONS

Aqueous-solution olivine mineral carbonation is a complex process. Key mechanisms that impact carbonation reactivity include passivating silica layer formation and cracking, silica surface migration, etch pit formation, inter-particle abrasion and the nucleation and growth of magnesite crystals on/in the silica/olivine reaction matrix. The Fe present in the host olivine is carried into the product carbonate, along with the Mg. The magnesite crystals appear to be able to both grow into and away from the olivine/silica reaction matrix, leaving boundary regions between the magnesite and the olivine/silica matrix that can facilitate further carbonate formation. Reaction interface regions have been observed to contain a structurally disrupted reaction front, which precedes mineral carbonation, underscoring the importance of olivine structural disruption during mineral carbonation. Passivating layer (e.g., silica) formation and inter-particle abrasion may play substantial roles hindering and enhancing carbonation reactivity, respectively. It is important to note the feedstock particles investigated herein were largely small single crystals. The impact of passivating surface layer formation and inter-particle abrasion on carbonation reactivity may differ substantially for olivine particles containing significantly higher concentrations of crystal defects. Investigations are planned to further explore the importance of and the mechanisms associated with passivating layer formation and particle abrasion.

ACKNOWLEDGMENTS

We gratefully acknowledge the National Energy Technology Laboratory of the U.S. Department of Energy for support through Grant # DE-FG26-01NT41282. We also thank the Center for Solid State Science for use of the Goldwater Materials Science Laboratories, including the Materials and Ion Beam Facilities and the Goldwater Materials Visualization Facility. We also acknowledge the Department of Chemistry and Biochemistry for the use of the X-ray Diffraction and Microprobe Facilities and the Center for Solid State Electronics Research for the use of the FESEM.

REFERENCES

1. Herzog, H.; Drake, E.; Adams, E. *CO_2 Capture, Reuse, and Storage Technologies for Mitigating Global Climate Change*, DOE Report No. DE-AF22-96PC01257 (1997).
2. *Carbon Sequestration Research and Development*, Offices of Science and Fossil Energy, U.S. Department of Energy (December 1999).
3. Current estimates of world coal reserves are 10,000 billion tons. Less than 0.1% is currently consumed annually (see references 4 and 5).
4. United Nations, *1991 Energy Statistics Yearbook*, New York, 1993.
5. Climate Change 1995: *The Science of Climate Change*. Contribution of Working Group I to the Second Assessment Report of the Intergovernmental Panel on Climate Change, Cambridge University Press, 1995.
6. Halmann, M.; Steinberg, M. *Greenhouse Gas Carbon Dioxide Mitigation, Science and Technology*, Lewis Publishers, London, 1999.
7. Seifritz, W. *Nature* 345, 486 (1990).
8. Lackner, K.; Wendt, C.; Butt, D.; Joyce Jr., E.; Sharp, D.; *Energy* 20, 1153-70 (1995).
9. O'Connor, W.; Dahlin, D.; Nilsen, D.; Walters, R.; Turner, P. *Proc. 25th Int. Tech. Conf. Coal Util. & Fuel Syst.* pp. 153-64 (2000).
10. O'Connor, W.K.; Dahlin, D.C.; Nilsen, D.N.; Gerdemann, S.J.; Rush, G.E.; Walters, R.P.; Turner, P.C. *Proc. 27th Int. Tech. Conf. Coal Util. & Fuel Syst.* pp. 819-30 (2002).
11. Yu, S.C.; Proc. Nat. Sci. Counc. A. ROC, 21, 173 (1997).
12. Ottonello, G.; Princivalle, F.; Della Giusta, A.; *Phys. Chem. Miner.* 17, 301 (1990).
13. Sample provided by D. Dahlin and W. O'Connor, Albany Research Center, Albany, Oregon.
14. Hurlbut, Cornelius, S.; Klein, Cornelis; *Manual of Mineralogy*, 19th Edition (John Wiley & Sons, New York, 1977).
15. Weast, Robert C., et al Eds.; *Handbook of Chemistry and Physics*, 54th Edition (CRC Press, Cleveland, Ohio, 1973).
16. Wells, A. F. *Structural Inorganic Chemistry*; 5th Edition (Clarendon Press: Oxford, 1984), p. 1293.
17. Chizmeshya, A.V.G.; McKelvy, M.J.; Wolf, G.; Kocher, M.; Gormley, D.; *Proc. 28th Int. Tech. Conf. Coal Util. & Fuel Syst.* (2003) following article.